SUPPLEMENTAL ONLINE MATERIAL

Bi-directional modulation of incubation of cocaine craving by silent synapse-based remodeling of prefrontal cortex to accumbens projections

Yao-Ying Ma, Brian R. Lee, Xiusong Wang, Changyong Guo, Lei Liu, Ranji Cui,
Yan Lan, Judith J. Balcita-Pedicino, Marina E. Wolf, Susan R. Sesack,
Yavin Shaham, Oliver M. Schlüter, Yanhua H. Huang, Yan Dong

Summary of the main results

	IL-to-NAcSh Projection	PrL-to-NAcCo Projection
Withdrawal day 1	**Generation of silent synapses** % silent synapses ↑	**Generation of silent synapses** % silent synapses ↑
Withdrawal day 45	**Unsilencing of silent synapses by insertion of CP-receptors** • % silent synapses back to control levels • Rectification index ↑ • Sensitivity to Naspm ↑ • Reemergence of silent synapses by Naspm +	**Unsilencing of silent synapses by insertion of nonCP-receptors** • % silent synapses back to control levels • Rectification index – • Sensitivity to Naspm – • Reemergence of silent synapses by Naspm – • Reemergence of silent synapses by LTD +
	Reversing silent synapse-based remodeling by LTD LTD: only occurs in cocaine-exposed rats. NMDAR-and mGluR1-dependent Loss of Naspm-sensitivity after LTD stimulation both in vitro and in vivo In vivo LTD: cue-induced cocaine seeking: ↑	**Reversing silent synapse-based remodeling by LTD** LTD: only occurs in cocaine-exposed rats. NMDAR-dependent, mGluR1-independent Re-emergence of silent synapses after LTD in vitro and in vivo In vivo LTD: cue-induced cocaine seeking: ↓

↑, increased; ↓, decreased; –, no changes; +, positive results

Detailed Experimental Procedures

Subjects

Male Sprague-Dawley rats (Charles River), postnatal day 28-30 at the beginning of the experiments were used. Rats were single housed under a 12 hr light/dark cycle (on at 700, off at 1900). Temperature (22 ± 1°C) and humidity (60 ± 5%) were controlled. The rats were used in all experiments in accordance with protocols approved by the Institutional Animal Care and Use Committees at University of Pittsburgh and European Neuroscience Institute.

Viral vectors

Recombinant adeno-associated vectors (rAAV2) expressing venus tagged ChR2 H134R were pseudotyped with AAV1/2 capsid proteins. HEK293T cells were co-transfected with the plasmids pF6 (adenoviral helper plasmid), pRVI (cap and rep genes for AAV serotype 2), pH21 (cap gene for AAV serotype 1 and rep gene for serotype 2) and the rAAV plasmid, using linear polyethylenimine assisted transfection. The helper plasmids were provided by Dr. M. Schwarz. Cultures grown in DMEM (Biochrom) with 10% substituted FBS (Biochrom, #S0115) were harvested from 15 by 15 cm dishes after 48h. rAAV were isolated and purified as described previously (Lee et al., 2013). The ChR2 gene was packaged with a YFP gene into a recombinant, replication-defective form of the adenovirus (AAV).

Imaging procedures

To verify the differential projections of the IL and PrL (Brog et al., 1993), we used the retrograde tract-tracing agent, Fluoro-Gold (FG; Fluorochrome, LLC) (Chang et al., 1990; Schmued and Fallon, 1986). Rats were anesthetized with a ketamine/xylazine mixture (50/5 mg/kg, i.p.) and placed in a stereotaxic apparatus (Stoelting). FG solution (2% in 0.1 M cacodylate buffer, pH 7.5) was injected iontophoretically (+2 µA, 7s on/7s off, 5 min) into the NAcSh or NAcCo with a glass micropipette (tip diameter: 10-15 µm). The coordinates used to target the NAcSh and NAcCo were, respectively, (in mm): +1.2 (AP), ±0.8 (ML) and -7.5 (DV, from skull surface) and +1.20 (AP), +1.45 (ML) and -6.80 (DV). After 5-7 days, rats were perfused transcardially with 100 U/ml heparin saline followed by 4% paraformaldehyde in 0.1 M phosphate buffer, pH 7.4 (PB). Brains were removed carefully, blocked coronally in 5-6 mm pieces, and given an additional 30-60 min postfix in 4% paraformaldehyde. Coronal sections through the PFC and NAc were cut at 50 µm with a vibrating microtome and collected into PB. One set of sections at 300 µm intervals (i.e. every sixth section) was mounted onto glass slides, dehydrated and coverslipped with Cytoseal 60 mounting medium. These sections were examined on an Olympus BX51 fluorescence microscope for injection site placement and extent of retrograde transport to the cortex. Only cases involving injections that were relatively confined to the NAcCo or NAcSh and that produced labeled cortical neurons were chosen for quantitative analysis. Of 16 rats, 5 involving primarily the NAcCo and 4 involving mainly the NAcSh were utilized.

For these cases, two additional sets of every sixth section were collected adjacent to those examined by fluorescence. One set was mounted on glass slides, stained for Nissl substance using Thionin, and then dehydrated and coverslipped with DPX mounting medium. The adjacent tissue set was processed by immunoperoxidase labeling for FG as follows. Sections were transferred to 0.1 M tris-buffered saline, pH 7.6 (TBS), blocked for 30 min in 1% BSA, 3% normal goat serum and 0.3% Triton-X 100 in TBS, and then incubated overnight (15 hours) in rabbit anti-FG antibody (1:4000, Chemicon) made in the blocking solution. Tissue was then rinsed in TBS and transferred to 1:400 biotinylated goat anti-rabbit IgG for 30 min, rinsed again and then incubated for 30 min in 1:200 avidin-biotin peroxidase complex (ABC Elite, Vector Labs). After a final rinse, bound peroxidase was visualized by treatment for 3.5 min in 0.02% 3,3'-diaminobenzidine and 0.003% hydrogen peroxide in TBS, and the reaction was stopped by extensive rinsing. Sections were then mounted onto glass slides, dehydrated, and coverslipped with DPX.

To quantify FG labeled neurons in the 9 chosen cases, the Stereo Investigator program from MicroBrightField was used in a manual mode to create cell maps within the IL and PrL. To avoid bias in selecting the border between the IL and the PrL, the boundaries of these two regions were first drawn on the adjacent Nissl stained sections (**Fig. 1A**) using the cytoarchitectonic criteria of Krettek and Price (Krettek and Price, 1977). The binary image of the boundaries was then superimposed onto the closest matching immunoperoxidase sections, adjusting only the medial and lateral boundaries to fit the edge of the tissue and the forceps minor, respectively. The IL and PrL regions were then examined systematically at a higher magnification, and all FG-labeled cells with clearly distinguishable nuclei were counted within these regions and within the section thickness. The granular nature of retrogradely transported FG greatly facilitated the identification of labeled cells (**Fig. 1B**, insert). The program provided the section thickness and areas of each binary trace, and the number of FG-positive neurons was then expressed as a density measure within the total volume of the IL and PL sampled.

For imaging of ChR2-YFP, rats were injected with AAV-ChR2-YFP into the subregions of the mPFC (**Fig. 1E,F**; see below viral injection). After approximately 3 weeks, rats were transcardially perfused and coronal sections (50 µm) were obtained as described above. Expression of ChR2-YFP in the mPFC and NAc was examined using BX51WIF microscope with 5x (**Fig. 1E,F**) and Leica SP5 confocal microscope with 40x (**Fig. 1G,H**) and 100x magnification (**Fig. 1I,J**).

Behavioral studies

Drugs

Cocaine HCl (Provided by NIDA Drug Supply Program) was dissolved in 0.9% NaCl saline. Ketamine and xylazine were mixed for anesthesia. Pentobarbital sodium was purchased from DEA-designated vendor at the University of Pittsburgh.

Definition of the IL and PrL, and viral delivery

The rodent mPFC is divided into a dorsal region PrL cortex and a ventral region IL cortex. There are no clearly anatomical boundaries that can be used, particularly in brain slices prepared for electrophysiological recording, to delineate these two subregions. Similar to many previous studies (Bossert et al., 2011; Bossert et al., 2012; Koya et al., 2009; LaLumiere et al., 2010; Peters et al., 2008), we targeted the dorsomedial PFC as the PrL, which may include the dorsal region of the PrL and possibly a small portion of the anterior cingulate cortex, and the ventromedial PFC as the IL, which may include the IL and possibly a small portion of the ventral portion of the PrL.

A 26 gauge injection needle was used to bilaterally inject 1 µl/site (0.2 µl/min) of the AAV2-ChR2-YFP solution via Hamilton syringe into the ventral regions of the mPFC (IL) (in mm: AP, +3.00; ML, ±0.70; DV, -4.75), or the dorsal regions of the mPFC (PrL) (in mm: AP, +3.00; ML, ±0.75; DV, -4.00), using a Thermo Orion M365 pump. Injection needles were left in place for 5 min following injection. ChR2-YFP was given 1-2 weeks before any experimental manipulations to ensure sufficient infection. Therefore, electrophysiological analyses were conducted ~3 weeks (1 d withdrawal) or ~8 weeks (45 d withdrawal) post infection.

Catheter Implantation

Self-administration surgery was as described previously (Brown et al., 2011; Mu et al., 2010). Briefly, a silastic catheter was inserted into the right jugular vein, and the distal end was led subcutaneously to the back between the scapulae. Catheters were constructed from silastic tubing (~8 cm; inner diameter 0.020 in, outer diameter 0.037 in) connected to a Quick Connect Harness (SAI Infusion). Rats were allowed to recover for 5-14 days. During recovery, the catheter was flushed daily with 1 ml/kg body weight of heparin (10 U/ml) and gentamicin antibiotic (5 mg/ml) in sterile saline to help protect against infection and catheter occlusion.

Self-administration apparatus

Experiments were conducted in operant-conditioning chambers enclosed within sound-attenuating cabinets (Med Associates). Each chamber contains an active and inactive nose poke, a food dispenser, the conditioned stimulus (CS) light in each nose poke and a house light. No food or water was provided in the chambers during the training or testing sessions.

Intravenous cocaine self-administration training

Cocaine self-administration training began 5-14 days after surgery. On day 1, rats were placed in the self-administration chamber for an overnight training session on a fixed ratio (FR) 1 reinforcement schedule. Nose poking in the active hole resulted in a cocaine infusion (0.75 mg/kg over 3-6 sec) and illumination of a CS light inside the nose poke hole. The CS light remained on for 6 sec, whereas the house light was illuminated for 20 sec during which active nose-pokes were counted but resulted in no cocaine infusions. After the 20 sec, the house light was turned off, and the next nose-poke in the active hole resulted in a cocaine infusion. Nose-pokes in the inactive hole had no reinforced consequences but were recorded. Rats that received at least 40 cocaine rewards in the overnight session were allowed to self-administer cocaine for 2 hr for 5 consecutive days ~24 hr after the overnight training on an FR1 reinforcement schedule. Same or similar cocaine self-administration procedures/standards were used in our previous studies (Mu et al., 2010; Otaka et al., 2013; Suska et al., 2013). Animals that did not meet this standard (n = 5) were removed from subsequent 5-day self-administration training.

Note that this cocaine self-administration procedure is modified, and thus slightly different, from the one we previously used (Lee et al., 2013). Differences include: i) Rats used in previous studies were purchased from Harlan, whereas rats used in the current studies were purchased from Charles River; and ii) In previous studies, the fixed volume of cocaine solution, and thus fix infusion duration, was used for each infusion. As such the concentrations were adjusted by body weight every day during the training. In the present study, the concentration of cocaine was fixed. As such, the infusion volume, and thus the infusion duration varied every day during the training.

Measurement of cue-induced cocaine seeking after withdrawal

We assessed incubation of cue-induced cocaine craving in extinction tests (1 hr) conducted after 1 and 45 days of withdrawal from cocaine self-administration. During the test sessions, active nose-pokes resulted in contingent delivery of the CS light cue but not cocaine. For behavioral assays without electrophysiology, we used within-subject assessment of incubation (Lu et al., 2004); the same rats were tested for cue-induced cocaine seeking on withdrawal day 1 and 45. For electrophysiology experiments, we used between-subject assessment; different groups of rats were sacrificed on either withdrawal day 1 or 45 without the extinction tests.

Optogenetic procedures

Construction of Optical Neural Interface (ONI)

For *in vivo* optical control of mPFC projections, two 105-µm core optic fibers were modified for attachment to an internal cannula creating the Optical Neural Interface (ONI). When the ONI was secured *in vivo* to the guide cannula, the stripped fiber extended 1.0 mm past the tip of the cannula. This experimental set-up was based on a previously verified setup (Lee et al., 2013) with slight modifications. The ONI was secured in vivo to the cannula head-mount only during stimulation.

In vivo stimulation

The ONI was attached with an FC/PC adaptor to a 473 nm blue laser diode (IkeCool), and light pulses were generated through a stimulator (A-M Systems). Optic fiber light intensity was measured using a light sensor (Thor Labs – PM100) and light intensity was adjusted to ~10 mW. Prior to attaching the ONI to head-mount guide cannula, the rat was briefly sedated with isoflurane to allow smooth insertion and to prevent damage to the optic fibers. Once the rat was fully awake, an LTD protocol was administered (1 Hz blue light pulses were administered for 10 min; pulse duration, 1.0 ms) in their home cage. Once this 10-min LTD protocol was concluded, the rat was placed in the testing chamber within 1 min after the end of the LTD stimulation. Control rats were also briefly sedated with isoflurane and a sham optic fiber was attached to the head-mount guide cannula. Upon awakening, they remained in their home cage for 10 min and subsequently were placed into a testing chamber.

In vitro stimulation

All evoked responses were delivered using an IkeCool laser at 473 nM, ~10 mW, through the microscope's 40x objective. The duration of the light pulse was adjusted between 0.1 – 1 ms for evoked responses with amplitudes of EPSCs at 100 – 300 pA, and 0.01 – 0.1 ms for minimal stimulation-evoked responses.

Electrophysiological studies

Slice preparation

Before decapitation, the rats were anesthetized with isoflurane and subsequently transcardially perfused with 4°C cutting solution (in mM: 135 *N*-methyl-D-glucamine, 1 KCl, 1.2 KH_2PO_4, 0.5 $CaCl_2$, 1.5 $MgCl_2$, 20 choline-HCO_3, 11 glucose, pH adjusted to 7.4 with HCl, and saturated with 95% O_2 /5% CO_2). The rat was decapitated, and then the brain was removed and glued to a block before being sliced using a Leica VT1200s vibratome in 4°C cutting solution. Coronal slices of 300 µm thickness were cut such that the preparation contained the signature anatomical landmarks (e.g., the anterior commissure) that clearly delineate the NAc subregions. After allowing 1-2 hr for recovery, one slice was transferred from a holding chamber to a submerged recording chamber where it was continuously perfused with oxygenated aCSF maintained at 30 ± 1°C.

Drugs

D-Aminophosphonovaleric acid (D-APV) was used at a concentration of 50 µM to inhibit NMDAR-mediated responses. LY367385 (LY) was used at a concentration of 50 µM to inhibit metabotropic glutamate receptor 1 (mGluR1). Picrotoxin (100 µM) was used to inhibit $GABA_AR$-mediated responses. Spermine (100 µM) was added freshly to the internal solution to restore the endogenous polyamine that blocks GluA2-lacking AMPARs. 2, 3-Dioxo-6-nitro-1, 2, 3, 4-tetrahydrobenzo[*f*]quinoxaline-7-sulfonamide (NBQX) (5 µM) was used to inhibit AMPAR-mediated responses. 1-Naplhthylacetyl spermine trihydrochloride (Naspm) (200 µM) was used to selectively inhibit GluA2-lacking AMPARs. TTX (1 µM) was used to block voltage-gated sodium channels. APV, NBQX, TTX, and LY367385 were purchased from R & D Systems, and all other chemicals were purchased from Sigma-Aldrich.

Whole-cell recordings

Standard whole-cell current- or voltage-clamp recording were used with a MultiClamp 700B amplifier (Molecular Device). During recordings, slices were superfused with aCSF that was heated to 30 ± 1°C by passing the

solution through a feedback-controlled in-line heater (Warner Instruments) before entering the chamber. Recordings were made under visual guidance (40x, differential interference contrast optics) with electrodes (3-5 MΩ). Expression of ChR2-YFP in neurons or processes was verified using an Olympus BX51WI fluorescent/DIC microscope before recordings. The intracellular and extracellular solutions can be found in our published papers (Lee et al., 2013). For all recordings, series resistance was 8 to 14 MΩ and was left uncompensated. Series resistance was monitored continuously during all recordings, and a change beyond 15% resulted in exclusion of the cell from data analyses. Synaptic currents were recorded with a MultiClamp 700B amplifier (Molecular Devices), filtered at 3 kHz, amplified 5 times, and then digitized at 20 kHz with a Digidata 1440A analog-to-digital converter (Molecular Devices). The recording electrodes (3 – 5 MΩ) were filled with (in mM): 125 $CsCH_3O_3S$, 15 CsCl, 5 TEA-Cl, 0.4 EGTA, 20 Hepes, 2.5 Mg-ATP, 0.25 Na-GTP, 1 QX-314, pH 7.3. Recording bath solution contained (in mM): 119 NaCl, 2.5 KCl, 2.5 $CaCl_2$, 1.3 $MgCl_2$, 1 NaH_2PO_4, 26.2 $NaHCO_3$, and 11 glucose, saturated with 95% O_2 / 5% CO_2 at 31-2°C. Picrotoxin (100 µM) was included in aCSF to block $GABA_A$ unless specified. NBQX (5 µM) was included in aCSF in some experiments to AMPA receptor-mediated response as specified. Naspm (200 µM) was locally superfused onto the slice through a wide-bore pipette (~150 µm) placed near the recording area. In the local perfusion, a control line containing only bath solution was included.

Silent synapse recordings

Neurons in the NAc shell were randomly selected for recording. Minimal stimulation experiments were performed as previously reported (Huang et al., 2009; Isaac et al., 1995; Lee et al., 2013; Liao et al., 1995). After obtaining a small (<50 pA) EPSC at -70 mV, the duration of the light pulse was reduced in small increments to the point that failures vs. successes of synaptically evoked events (EPSCs) could be clearly distinguished visually. Pulse duration and frequency were then kept constant for the rest of the experiment. The amplitude of both AMPAR and NMDAR ESPCs resulting from single vesicle release is relatively large (e.g., ~15 pA for AMPAR mEPSCs) (Huang et al., 2009), which facilitates the judgment of success vs. failures of EPSCs; therefore, they were defined visually. For each cell, 50-100 traces were recorded at -70 mV, and 50-100 traces were recorded at +50 mV. Recordings were then repeated at -70 mV and +50 mV for another round or two. Each cell was recorded at least 2 rounds. Only cells with relatively constant failure rates (changes <10%) between rounds were included for calculation of % silent synapses.

We made two theoretical assumptions: 1) the presynaptic release sites are independent, and 2) release probability across all synapses, including silent synapses are identical. Thus, percent silent synapses were calculated using the equation: $1-Ln(F_{-70})/Ln(F_{+50})$, in which F_{-70} was the failure rate at -70 mV and F_{+50} was the failure rate at +50 mV, as rationalized previously (Liao et al., 1995). However, these two theoretical assumptions may not be true in our experimental conditions.

For example, the release probability at silent synapses may be different from that at regular synapses. In this case, we define the total number of synapses as "t", which is equal to the number of non-silent synapses ("n") and number of silent synapses ("s"). Thus, t = n + s. We define the prelease probability at non-silent synapses as Pn, and the release probability at silent synapses as Ps. At -70 mV, for a fixed number of synapses (t), the failure rate is exclusively determined by the release probability and the number of non-silent synapses, Pn: $F_{-70} = (1-Pn)^n$. At +50 mV, $F_{+50} = (1-Pn)^n(1-Ps)^s$. These two equations can be transferred to: (1) $Ln(F^{-70}) = nLn(1-Pn)$; and (2) $Ln(F^{+50}) = nLn(1-Pn) + sLn(1-Ps)$. Thus, (3) $n = Ln(F_{-70})/Ln(1-Pn)$; and (4) $s = [Ln(F_{+50}) - Ln(F_{-70})]/Ln(1-Ps)$. Let $(1-Ps) = (1-Pn)^a$ then (4) will be: (5) $s = [Ln(F_{+50}) - Ln(F_{-70})]/aLn(1-Pn)$.

As such, the number of silent synapses over the number of total synapses should be: $s/t = s/(s+n)=(5)/[(5)+(3)] = \{[Ln(F_{+50})-Ln(F_{-70})]/aLn(1-Pn)\}/\{[Ln(F_{+50})-Ln(F_{-70})]/aLn(1-Pn) +Ln(F_{-70})/Ln(1-Pn)\}$. After reorganization, (6) $s/t = [Ln(F_{+50}) – Ln(F_{-70})]/\{Ln(F_{+50})-(1-a)Ln(F_{-70})]$, in which $(1-Ps) = (1-Pn)^a$. Thus, if Ps = Pn, $a = Ln(1-Ps)/Ln(1- Pn) = 1$, and (6) can be converted to the original equation $s/t = 1-Ln(F_{-70})/Ln(F_{+50})$. If Ps > Pn, then a <1, and thus the s/t assessed by (6) will be higher than that assessed by the original equation. Similarly, if Ps< Pn, then a >1, and the s/t assessed by (6) will be lower than that assessed by the original equation. Thus, if the release probability differs between silent and non-silent synapses, the actual % silent synapses reported in this study should be higher or lower than the actual %. However, as demonstration during the derivation process, this only introduces quantitative errors, and should not qualitatively affect the results. In other word, the fact that cocaine exposure increases % silent synapses is not affected by this assessment error.

The major difference between minimal stimulations delivered by optical fibers and electrical electrode is that electrical stimulation can be confined to one or a few afferents around the well-defined stimulation site (i.e., the tip of the stimulation electrode), whereas minimal optical stimulation will preferentially influence the afferents with the highest expression of ChR2 despite not necessarily being located together. This difference may not be a major concern because: i) the amplitudes of successful synaptic responses elicited by minimal optical

stimulations are similar or very close to that of mEPSCs (see example traces throughout the manuscript), suggesting that one or very few afferents are stimulated each time. Thus, the premise that only a very small number of synapses are activated each time is met, even without knowing the actual activation spot; ii) Given that only fibers with the highest expression of ChR2 are activated with short-duration stimulation, we assume that this same set of fibers is repeatedly activated throughout the trial, similar to minimal electrical stimulation in which the same set of fibers that is most sensitive to electrical stimulation is assumed to be activated repeatedly; iii) When performing the minimal optical stimulation assay, the stimulation intensity/duration was adjusted such that failure rate was around 0.5 (ranging from 0.2 -0.8 with median of 0.5). Successes and failures were readily separable, with the pattern similar to that observed in previous studies detecting silent synapses (Huang et al., 2009; Isaac et al., 1995; Liao et al., 1995) using minimal electrical stimulation. Thus, even with potentially different properties of optical stimulation, the minimal optical stimulation can still detect silent synapses, at least semi-quantitatively.

Rectification of AMPAR EPSCs

To examine AMPAR subunit composition, an IV curve was plotted. Evoked PFC-to-NAc AMPAR-mediated EPSCs were measured at the membrane potentials of -70, -50, -30, -10, 0, 10, 30, 50, and 70 mV. The rectification index was calculated by comparing the peak amplitude at +70 mV to -70 mV after offsetting the reversal potential (Lee et al., 2013).

In vitro LTD recording

Light-evoked LTD was induced at IL-to-NAcSh or PrL-to-NAcCo synapses in cocaine- or saline-exposed rats. The LTD induction protocol (stimulation duration: 0.1-1 ms, consistent with that in baseline stimulation; frequency: 1 Hz; train duration: 10 min), was applied to the brain slices after a stable baseline of EPSCs was obtained from the same stimulation intensity except that the stimulation frequency was 0.1 Hz.

Data acquisition and analysis

In all electrophysiology experiments, the data were coded before analysis. Data were then de-coded for the final results. All results are shown as mean ± SEM. Each experiment was replicated in at least 4 rats (~1-4 cells were recorded from each rat) for electrophysiological analysis and 7 rats for behavioral tests. No data points were excluded unless specified in the experimental procedure. A total of 257 rats were used, among which 6 rats were excluded before data collection because of the catheter leakage or clogging, 9 rats were excluded before data collection because of surgery-associated infection or significant (>15%) loss of body weight, 11 rats were excluded during data collection because misplacement of cannulas (found during preparation of brain slices) or damages of optical fibers during in vivo stimulation, and 5 rats were excluded because they did not initiate cocaine self-administration.

Data from the repeated experiments for the same sub-study were pooled together for statistical analyses. Technical replicates were utilized for some of the key experiments, such as insertion of CP-AMPARs, in which biophysical (rectification of AMPAR EPSCs) and pharmacological (sensitivity to Naspm) approaches were both employed. Sample size for each experiment was determined either based on our previous experience with similar experiments or those that have been routinely used in similar studies published in this journal. Sample size in electrophysiology experiments was presented as n/m, where "n" refers to the number of cells examined and "m" refers to the number of rats. Normal distribution was assumed for all statistics. This is based on our previous work related to silent synapses, in which a typical normal distribution was observed (Brown et al., 2011). Variance was estimated for most major results and no significant difference was found between control and manipulation groups. Statistical significance was assessed using *t*-tests (when two groups are compared) or one/two-way ANOVAs (when multiple groups or repeated measured were involved), followed by Bonferroni post-hoc tests. For all experiments involving electrophysiology using treated animals, both cell- animal-based statistics were performed and reported, with results of cell-based analysis provided in graphic presentations. In animal-based analyses, electrophysiological parameters of all recorded cells from a single rat were averaged and the mean was used to represent this parameter of this rat for subsequent animal-based analysis.

Specific Experiments

Different physiological consequences by optogenetic stimulations with short and long laser duration

To selectively target cocaine-induced effects without affecting the basal transmission of the IL-to-NAcSh and PrL-to-NAcCo projections, we optimized a LTD induction protocol that did not affect the basal transmission of these two projections in saline-exposed rats but induced modest depression in cocaine-exposed rats. Our first

goal was to optimize a set of optogenetic stimulation parameter that can mimic electrical stimulation. Ideally, the stimulation should provide minimal but essential depolarization to activate sodium channels, which in turn triggers the action potential-synaptic release cascade, as happened under physiological conditions. We optimized a laser stimulation with short durations, i.e., 0.01 – 0.1 ms for the minimal stimulation assay and 0.1 - 1 ms for evoked EPSCs and LTD induction.

We show data validating these short duration protocols in the main manuscript. Here, we provide additional results showing that optogenetic stimulation with long duration generated artifacts that may result in different physiological consequences. ChR2 is a nonselective channel, conducting sodium, calcium and other cations once activated. Prolonged activation of ChR2 by long laser pulse (e.g., 4 ms) may result in additional electrophysiological consequences that are not normally present under physiological conditions. Specifically, optogenetic stimulation with longer laser duration induced larger depolarizing currents in ChR2-expressing neurons that are often resistant to TTX (**Fig. S1A-D**), suggesting a significant contribution of ions that directly pass through ChR2. This enhanced and prolonged conductance may result in prolonged depolarization. Accordingly, more than one action potential was often elicited by optogenetic stimulation with long laser pulses (**Fig. S1C,E**).

When activating presynaptic terminals that expressed ChR2, optogenetic stimulation with long laser pulses often elicited EPSCs with multiple components (**Fig. S1F**); this effect is likely due to multiple action potentials evoked presynaptically. Importantly, even in the presence of TTX, optogenetic stimulation of presynaptic terminals with long laser pulse could elicit EPSCs (**Fig. S1G-I**), indicating the involvement of action potential-independent mechanisms. Furthermore, other electrophysiological and biophysical parameters of EPSCs elicited by optogenetic stimulation with long laser duration were also not normal. Particularly, the variance of EPSCs tended to be smaller (**Fig. S1J,K**). In addition, likely due to prolonged activation and enhanced calcium influx, presynaptic release probability was also higher than normal (**Fig. S1L-P**).

Experiment 1**:** Generation of silent synapses within the IL-to-NAcSh and PrL-to-NAcCo projections after 1 day of withdrawal from cocaine self-administration (Figs. 2, 5)

We examined cocaine-induced generation of silent synapses within the IL-to-NAcSh or PrL-to-NAcCo projections from rats that were treated with the 6-day cocaine or saline self-administration procedure as described above. For all self-administration experiments in the manuscript, rats were bilaterally injected with AAV2-ChR2-YFP into the IL or PrL and then implanted with a silastic catheter into their right jugular vein. After approximately two weeks of recovery, self-administration training was conducted. Briefly, we trained the rats with one overnight session on an FR1 reinforcement schedule with either saline (the same vvolume of 0.9% saline as received by cocaine-exposed rats based on body weight) or cocaine HCl (0.75 mg/kg/infusion). If the rats had at least 40 cocaine infusions during the overnight session, they began 5 consecutive 2-hr training days under the same reinforcement schedule on the following day. After completing the 5-day training, the rats were used for electrophysiological analysis of silent synapses after 1 day of withdrawal in their home cages (saline self-administration, neurons/rats (n/m) = 12/5 for IL-to-NAcSh and 16/4 for PrL-to-NAcCo; cocaine self-administration, n/m = 10/4 for IL-to-NAcSh and 14/4 for PrL-to-NAcCo). To estimate the number of silent synapses, minimal stimulation experiments were performed. Optogenetic stimulation was used to obtain a small EPSC at IL-to-NAcSh or PrL-to-NAcCo synapses while holding the cells at -70mV. Then, the duration of the light pulse was reduced in small increments to a point at which failures vs. successes could be clearly defined. The recordings at the two membrane potentials were then repeated 1-2 rounds to ensure their stability. Responses immediately after (within 2.5 min) the change of holding potentials, were not included for analysis. Percent silent synapses were calculated using the equation: $1-Ln(F_{-70})/Ln(F_{+50})$, in which F_{-70} was the failure rate at -70 mV and F_{+50} was the failure rate at +50 mV (Huang et al., 2009).

Experiment 2**:** Maturation of silent synapses within the IL-to-NAcSh and PrL-to-NAcCo projections after 45 days of withdrawal from cocaine self-administration (Figs. 2, 3, 5, 6)

We first measured the levels of silent synapses within the IL-to-NAcSh or PrL-to-NAcCo projections from rats after 45 days of withdrawal from the cocaine or saline self-administration procedure as described above. Rats received bilateral injection of AAV2-ChR2-YFP into the IL or PrL and self-administration surgery before the training, as described above. After completing the 6-day training, the rats were returned to their homecages for a withdrawal period of 45 days. On withdrawal day 45, rats were used for electrophysiological analysis using the

optogenetic minimal stimulation assay as described in Experiment 1 (saline, n/m=16/9 for IL-to-NAcSh and 10/5 for PrL-to-NAcCo; cocaine, n/m=27/13 for IL-to-NAcSh and 12/5 for PrL-to-NAcCo).

We next measured the rectification of AMPAR EPSCs at IL-to-NAcSh or PrL-to-NAcCo synapses from rats after 45 days of withdrawal from the cocaine or saline self-administration procedures as described above. Rats received bilateral injections of AAV2-ChR2-YFP into the IL or PrL and self-administration surgery before the training, as described above. After completing the 6-day training, the rats were returned to their homecages for a withdrawal period of 45 days. On withdrawal day 45, rats were used for electrophysiological analysis using the optogenetic stimulation to elicit EPSCs from IL-to-NAcSh or PrL-to-NAcCo synapses (saline, n/m=12/6 for IL-to-NAcSh and 11/5 for PrL-to-NAcCo; cocaine, n/m=33/10 for IL-to-NAcSh and 9/6 for PrL-to-NAcCo).

We next measured the sensitivity of AMPAR EPSCs at IL-to-NAcSh or PrL-to-NAcCo synapses to Naspm from rats after 45 days of withdrawal from the cocaine or saline self-administration procedures as described above. Rats received bilateral injections of AAV2-ChR2-YFP into the IL or PrL and self-administration surgery before the training, as described above. After completing the 6-day training, the rats were returned to their homecages for a withdrawal period of 45 days. On withdrawal day 45, rats were used for electrophysiological analysis using the optogenetic stimulation to elicit EPSCs from IL-to-NAcSh or PrL-to-NAcCo synapses. Naspm was dissolved in regular aCSF and was delivered through local perfusion (different from bath application) (saline, n/m=13/8 for IL-to-NAcSh and 11/5 for PrL-to-NAcCo; cocaine, n/m=10/5 for IL-to-NAcSh and 11/5 for PrL-to-NAcCo).

We measured the levels of silent synapses within the IL-to-NAcSh or PrL-to-NAcCo projections in the presence of Naspm from rats after 45 days of withdrawal from the cocaine or saline self-administration procedure as described above. Rats received bilateral injection of AAV2-ChR2-YFP into the IL or PrL and self-administration surgery before the training, as described above. After completing the 6-day training, the rats were returned to their homecages for a withdrawal period of 45 days. On withdrawal day 45, rats were used for electrophysiological analysis using the optogenetic minimal stimulation assay (saline, n/m=9/6 for IL-to-NAcSh and 7/5 for PrL-to-NAcCo; cocaine, n/m=15/7 for IL-to-NAcSh and 9/5 for PrL-to-NAcCo).

Experiment 3: LTD at PFC-to-NAc synapses (Figs. 4, 7)

We first attempted to induce LTD at IL-to-NAcSh or PrL-to-NAcCo synapses from rats after 45 days of withdrawal from saline or cocaine self-administration. The self-administration procedures were identical to the ones used in Experiment 1. Experiments were performed on withdrawal day 45. Light pulses, 0.1-1 ms in duration, were used to evoke PFC-to-NAc EPSCs while holding the cell at -70mV. Once a stable baseline was obtained for ~10 min, a light–evoked LTD-induction protocol was administered: 0.1-1-ms flashes, 1 Hz for 10 min to IL-to-NAcSh or PrL-to-NAcCo synapses, with the holding potential of -50mV (upstate potentials) where striatal neurons spend most of their time in behaving rats(Mahon et al., 2006). Following this induction, recordings were continued for at least 30 min at -70mV (saline, n/m=10/7 for IL-to-NAcSh and 9/5 for PrL-to-NAcCo; cocaine, n/m=11/6 for IL-to-NAcSh and 10/5 for PrL-to-NAcCo).

We next examined the sensitivity of EPSCs from IL-to-NAcSh or PrL-to-NAcCo synapses to Naspm after LTD from rats after 45 days of withdrawal from saline or cocaine self-administration (saline, n/m=9/7 for IL-to-NAcSh and 9/5 for PrL-to-NAcCo; cocaine, n/m=11/6 for IL-to-NAcSh and 9/5 for PrL-to-NAcCo). The self-administration procedures were identical to the ones used in Experiment 1. Experiments were performed on withdrawal day 45. 10-30 min after LTD induction, Naspm (200 µM) was applied through the local perfusion system for ~10 min.

We then examined the potential induction mechanisms underlying LTD of IL-to-NAcSh and PrL-to-NAcCo transmission from rats after 45 days of withdrawal from cocaine self-administration (APV, n/m=12/5 for IL-to-NAcSh and 9/5 for PrL-to-NAcCo; LY, n/m=13/4 for IL-to-NAcSh and 10/5 for PrL-to-NAcCo;). The self-administration procedures were identical to the ones used in Experiment 1. For either IL-to-NAcSh or PrL-to-NAcCo synapses, recordings were performed as described above for the LTD experiment except that either D-APV (50 µM) or LY (50 µM) was added to the bath.

Experiment 4: Effect of in vivo LTD on cue-induced cocaine seeking on withdrawal day 45 (Fig. 8)

We used two groups of rats to examine IL-to-NAcSh and PrL-to-NAcCo projections, respectively. These rats received the cocaine self-administration procedures and intra-IL or intra-PrL injection of ChR2-expressing virus as described above. These rats were tested for extinction responding (1-h session) on withdrawal days 1 and 45. On withdrawal day 35 rats were anesthetized with sodium pentobarbital (40 mg/kg) and placed in a stereotaxic apparatus. A bilateral 26 gauge guide cannula was inserted 1.0 mm above the NAcSh (IL-to-NAcSh in mm: AP, +1.55; ML, ±0.60; DV, -6.00) or core (PrL-to-NAcCo group in mm: AP, +1.40; ML, ±1.50; DV, -5.50) and secured with cranial screws and dental cement. On withdrawal day 45, the rats were divided into two subgroups: one subgroup had a sham optic fiber inserted into the guide cannula; the other group received a true optic fiber-ONI. The ONI was adjusted to a power level of ~10 mW at the optic fiber tip and the rat was briefly anesthetized to allow smooth insertion of optic fiber.

Sham controls received the same brief anesthesia and installation of optical fiber. Once the rats recovered and were freely moving, we initiated the LTD protocol with an IkeCool laser connected to a pulse generator (1 Hz for 10 min) in the rats' home cages. The sham control group received an identical treatment except that the optic fiber was not functional. After the LTD stimulation train was completed, some rats were used for checking the in vivo efficacy of the LTD protocol (saline, n/m=12/4 for IL-to-NAcSh and 17/5 for PrL-to-NAcCo; cocaine, n/m=15/4 for IL-to-NAcSh and 20/5 for PrL-to-NAcCo), and other rats were placed in the operant chamber for a 1-hr extinction test (sham, n=13 for IL-to-NAcSh and n=9 for PrL-to-NAcCo; cocaine, n=11 for IL-to-NAcSh and n=9 for PrL-to-NAcCo).

To assess the potential nonspecific effects of in vivo LTD within the PrL-to-NAcCo projection (which drove the level of cocaine seeking at withdrawal day 45 below the level at withdrawal day 1), we examined the effects of this projection-specific LTD on sucrose self-administration. Briefly, ~14 days after bilateral injection of AAV2-ChR2-YFP into the PrL and cannulation in the NAcCo, we trained rats to self-administer (nosepoke) sucrose pellets (45 mg) under the same experimental conditions (session duration and reinforcement schedule) we used in the cocaine self-administration studies. The rats were food restricted in their home cage with the body weight maintained ~95% of their original values. Rats received a 10-min in vivo LTD protocol as described in the main manuscript to the PrL-to-NAcCo projection on training day 6, followed (1 min after) by the training session. We found that the in vivo LTD induction had no effect on sucrose self-administration; there were no differences in nosepoke responding and number of sucrose deliveries between the training day prior to the in vivo LTD induction and the test day (**Fig. S3F**).

Supplementary Figure Legends

Figure S1 Different electrophysiological membrane consequences of optogenetic stimulation with short and long stimulation durations. A Example whole-cell currents in a ChR2-expressing PrL neuron elicited by a short (1 ms, black) and a long (4 ms, red) laser pulse. Voltage-clamp recordings were made at -70 mV. **B** The same recordings but performed in the presence of TTX (1 μM) showing that inhibition of sodium channels (by TTX) much reduced the whole-cell current evoked by the short laser pulse but a significant amount of current still remained if evoked by the 4-ms laser pulse. These results suggest that the laser-induced current by the 1-ms pulse was mainly sodium channel-mediated, and triggered by the initial depolarization mediated by ChR2. In contrast, the large current evoked by the 4-ms laser pulse was partially mediated by ChR2 itself. **C** Example traces from whole-cell current-clamp recording showing that the 1-ms laser pulse reliably induced a single action potential, whereas double action potentials were often evoked by the 4-ms laser pulse. **D** Example whole-cell currents in a ChR2-expressing IL neuron elicited by a short (1 ms, black) and a long (4 ms, red) laser pulse. Voltage-clamp recordings were made at -70 mV. Inset: The same recordings but performed in the presence of TTX (1 μM) showing that inhibition of action potential firing (by TTX) inhibited most current evoked by the short laser pulse but a significant amount of current still remained if evoked by the 4-ms laser pulse. **E** Example traces from whole-cell current-clamp recording showing that the 1-ms laser pulse reliably induced a single action potential, whereas double action potentials were often evoked by the 4-ms laser pulse. **F** Example synaptic responses within the IL-to-NAcSh projection elicited by a 1-ms (black) and a 4-ms (red) laser pulse. Multiple components were often observed in synaptic responses elicited by the 4-ms laser pulse, consistent with the observation that the 4-ms laser pulse often evoked multiple action potentials in ChR2-expressing neurons. **G** and **H** Example synaptic responses at IL-to-NAcSh (**G**) or PrL-to-NAcCo (**H**) synapses elicited by a 1-ms (black) or 4-ms (red) laser pulse in the presence of TTX (1 μM). Prolonged (e.g., 4 ms) optogenetic stimulation elicited nonphysiological, action potential-independent synaptic transmission. **I** Summarized results showing that at the same recorded IL-to-NAcSh (1 ms, 6.7 ± 1.6; 4 ms, 36.0 ± 10.8, n = 5, $t_{(4)} = 2.8$, p = 0.04, paired t-test) or PrL-

to-NAcCo (1 ms, 10.0 ± 0.8; 4 ms, 43.9 ± 8.7, n = 5, $t_{(4)}$ = 3.8, p = 0.02, paired t-test) synapses, prolonged (i.e., 4 ms) optogenetic stimulation elicited TTX-independent EPSCs that were not observed after short optogenetic stimulation or electrical stimulation. **J** and **K** Trials of recordings of IL-to-NAcSh (**E**) or PrL-to-NAcCo (**F**) synaptic transmission elicited first by 1-ms laser pulses (black) followed by 4-ms laser pulses (red). Responses elicited by 4-ms laser pulses exhibited reduced variation, suggesting increased presynaptic release probability. **L** Five consecutive synaptic responses within the IL-to-NAcSh projection elicited by 1-ms (upper, black) or 4-ms (lower, red) laser pulses at 20 Hz. **M** The relationship of the variance vs. mean of the EPSC amplitudes of the same cells. **N** Five consecutive synaptic responses within the PrL-to-NAcCo projection elicited by 1-ms (upper, black) or 4-ms (lower, red) laser pulses at 20 Hz. **O** The relationship of the variance vs. mean of the EPSC amplitudes of the same cells. **P** Summarized results showing that the release probability of 4-ms laser pulse-induced synaptic responses (IL-to-NAcSh, 0.79 ± 0.04, n = 5, $t_{(4)}$ = 4.6, p = 0.01, paired t-test; PrL-to-NAcCo, 0.56 ± 0.11, n = 5, $t_{(4)}$ = 5.7, p < 0.01), estimated by the Variance vs. Mean analysis, was significantly higher than synaptic responses elicited by 1-ms laser pulses (0.55 and 0.38) or electrical stimulation (0.3 – 0.5).

Figure S2 Additional experimental results associated with Figure 2-7 in the main text.
A-D Summarized results show saline or cocaine self-administration training of rats that were used for Figure 2. **E** Summarized results show saline or cocaine self-administration training of rats that were used for Figure 3. **F-G** Summarized results show saline or cocaine self-administration training of rats that were used for Figure 4. **H-K** Summarized results show saline or cocaine self-administration training of rats that were used for Figure 5. **L** Summarized results show saline or cocaine self-administration training of rats that were used for Figure 6. **M-O** Summarized results show saline or cocaine self-administration training of rats that were used for Figure 7.

Figure S3: Additional experimental results associated with Figure 8. A Summarized results show saline or cocaine self-administration training of rats that were used for Figure 8B,C. **B** Summarized results show saline or cocaine self-administration training of rats that were used for Figure 8E-I. **C** Summarized results show cocaine self-administration training of rats that were used for Figure 8D. **D** Summarized results show cocaine self-administration training of rats that were used for Figure 8J. **E** Diagrams of coronal slices showing the cannulation sites (solid, LTD; open, sham) in the NAcSh and NAcCo. **F** Summarized results showing that rats with intra-PrL expression of ChR2 exhibited stable sucrose self-administration over the 7-day session (2 h/session). Application of the LTD protocol to PrL-to-NAcCo projection in vivo on day 6 (1 min before the self-administration session) did not affect subsequent sucrose self-administration (day 5 vs. day 6 x LTD vs. sham: $F_{(1,12)}$ = 0.35, p = 0.56, two-way ANOVA).

Figure S4: Graphic summary of cocaine-induced silent synapse-based circuitry remodeling. A Diagram showing that in naïve rats, the NAcCo and NAcSh receive synaptic inputs from the PFC and BLA, with PrL mPFC preferentially projecting to NAcCo and IL mPFC preferentially projecting to NAcSh. Note that the BLA projection to NAcCo is not depicted because silent synapse-based circuitry remodeling in this projection has yet to be investigated. The basal transmission within these projections may be essential for certain aspects of cocaine craving and relapse. **B** Diagram showing that cocaine exposure (measured at withdrawal day 1 after cocaine self-administration) generates AMPAR-silent synapses within at least three NAc efferents, PrL-to-NAcCo, IL-to-NAcSh, and BLA-to-NAcSh projections. Silent synapses may be generated on pre-existing projection fibers (as diagrammed in the PrL and BLA projections) or on newly sprouted presynaptic fibers (as diagramed in the IL projection). **C** Diagram showing that after withdrawal from cocaine, silent synapses within each projection may mature via different cellular processes. Specifically, silent synapses within the PrL-to-NACo projection mature by recruiting typical calcium-impermeable AMPARs (CI-AMPARs), whereas silent synapses within the IL- and BLA-to-NAcSh projections mature by recruiting atypical CP-AMPARs. Via generation and maturation of silent synapses, these projections are remodeled and are hypothesized to form new circuits that control or regulate incubation of cocaine craving after prolonged withdrawal. Using in vivo LTD induction, we were able to selectively reverse the maturation step of silent synapse-based remodeling of each projection and reveal their role in incubation of cocaine craving. Our results suggest that silent synapse-based remodeling of the PrL-to-NAco and BLA-to-NAcSh projections promotes incubation of cocaine craving, whereas remodeling of the IL-to-NAcSh projection counteracts/inhibits incubation of cocaine craving.

References

Bossert, J.M., Stern, A.L., Theberge, F.R., Cifani, C., Koya, E., Hope, B.T., and Shaham, Y. (2011). Ventral medial prefrontal cortex neuronal ensembles mediate context-induced relapse to heroin. Nat Neurosci 14, 420-422.

Bossert, J.M., Stern, A.L., Theberge, F.R., Marchant, N.J., Wang, H.L., Morales, M., and Shaham, Y. (2012). Role of projections from ventral medial prefrontal cortex to nucleus accumbens shell in context-induced reinstatement of heroin seeking. The Journal of neuroscience : the official journal of the Society for Neuroscience 32, 4982-4991.

Brog, J.S., Salyapongse, A., Deutch, A.Y., and Zahm, D.S. (1993). The patterns of afferent innervation of the core and shell in the "accumbens" part of the rat ventral striatum: immunohistochemical detection of retrogradely transported fluoro-gold. J Comp Neurol 338, 255-278.

Brown, T.E., Lee, B.R., Mu, P., Ferguson, D., Dietz, D., Ohnishi, Y.N., Lin, Y., Suska, A., Ishikawa, M., Huang, Y.H.*, et al.* (2011). A silent synapse-based mechanism for cocaine-induced locomotor sensitization. The Journal of neuroscience : the official journal of the Society for Neuroscience 31, 8163-8174.

Chang, H.T., Kuo, H., Whittaker, J.A., and Cooper, N.G. (1990). Light and electron microscopic analysis of projection neurons retrogradely labeled with Fluoro-Gold: notes on the application of antibodies to Fluoro-Gold. Journal of neuroscience methods 35, 31-37.

Huang, Y.H., Lin, Y., Mu, P., Lee, B.R., Brown, T.E., Wayman, G., Marie, H., Liu, W., Yan, Z., Sorg, B.A.*, et al.* (2009). In vivo cocaine experience generates silent synapses. Neuron 63, 40-47.

Isaac, J.T., Nicoll, R.A., and Malenka, R.C. (1995). Evidence for silent synapses: implications for the expression of LTP. Neuron 15, 427-434.

Koya, E., Uejima, J.L., Wihbey, K.A., Bossert, J.M., Hope, B.T., and Shaham, Y. (2009). Role of ventral medial prefrontal cortex in incubation of cocaine craving. Neuropharmacology 56 Suppl 1, 177-185.

Krettek, J.E., and Price, J.L. (1977). The cortical projections of the mediodorsal nucleus and adjacent thalamic nuclei in the rat. The Journal of comparative neurology 171, 157-191.

LaLumiere, R.T., Niehoff, K.E., and Kalivas, P.W. (2010). The infralimbic cortex regulates the consolidation of extinction after cocaine self-administration. Learn Mem 17, 168-175.

Lee, B.R., Ma, Y.Y., Huang, Y.H., Wang, X., Otaka, M., Ishikawa, M., Neumann, P.A., Graziane, N.M., Brown, T.E., Suska, A.*, et al.* (2013). Maturation of silent synapses in amygdala-accumbens projection contributes to incubation of cocaine craving. Nat Neurosci 16, 1644-1651.

Liao, D., Hessler, N.A., and Malinow, R. (1995). Activation of postsynaptically silent synapses during pairing-induced LTP in CA1 region of hippocampal slice. Nature 375, 400-404.

Lu, L., Grimm, J.W., Dempsey, J., and Shaham, Y. (2004). Cocaine seeking over extended withdrawal periods in rats: different time courses of responding induced by cocaine cues versus cocaine priming over the first 6 months. Psychopharmacology 176, 101-108.

Mahon, S., Vautrelle, N., Pezard, L., Slaght, S.J., Deniau, J.M., Chouvet, G., and Charpier, S. (2006). Distinct patterns of striatal medium spiny neuron activity during the natural sleep-wake cycle. The Journal of neuroscience : the official journal of the Society for Neuroscience 26, 12587-12595.

Mu, P., Moyer, J.T., Ishikawa, M., Zhang, Y., Panksepp, J., Sorg, B.A., Schluter, O.M., and Dong, Y. (2010). Exposure to cocaine dynamically regulates the intrinsic membrane excitability of nucleus accumbens neurons. The Journal of neuroscience : the official journal of the Society for Neuroscience 30, 3689-3699.

Otaka, M., Ishikawa, M., Lee, B.R., Liu, L., Neumann, P.A., Cui, R., Huang, Y.H., Schluter, O.M., and Dong, Y. (2013). Exposure to cocaine regulates inhibitory synaptic transmission in the nucleus accumbens. The Journal of neuroscience : the official journal of the Society for Neuroscience 33, 6753-6758.

Peters, J., LaLumiere, R.T., and Kalivas, P.W. (2008). Infralimbic prefrontal cortex is responsible for inhibiting cocaine seeking in extinguished rats. The Journal of neuroscience : the official journal of the Society for Neuroscience 28, 6046-6053.

Schmued, L.C., and Fallon, J.H. (1986). Fluoro-Gold: a new fluorescent retrograde axonal tracer with numerous unique properties. Brain research 377, 147-154.

Suska, A., Lee, B.R., Huang, Y.H., Dong, Y., and Schluter, O.M. (2013). Selective presynaptic enhancement of the prefrontal cortex to nucleus accumbens pathway by cocaine. Proc Natl Acad Sci U S A 110, 713-718.

Fig. S1

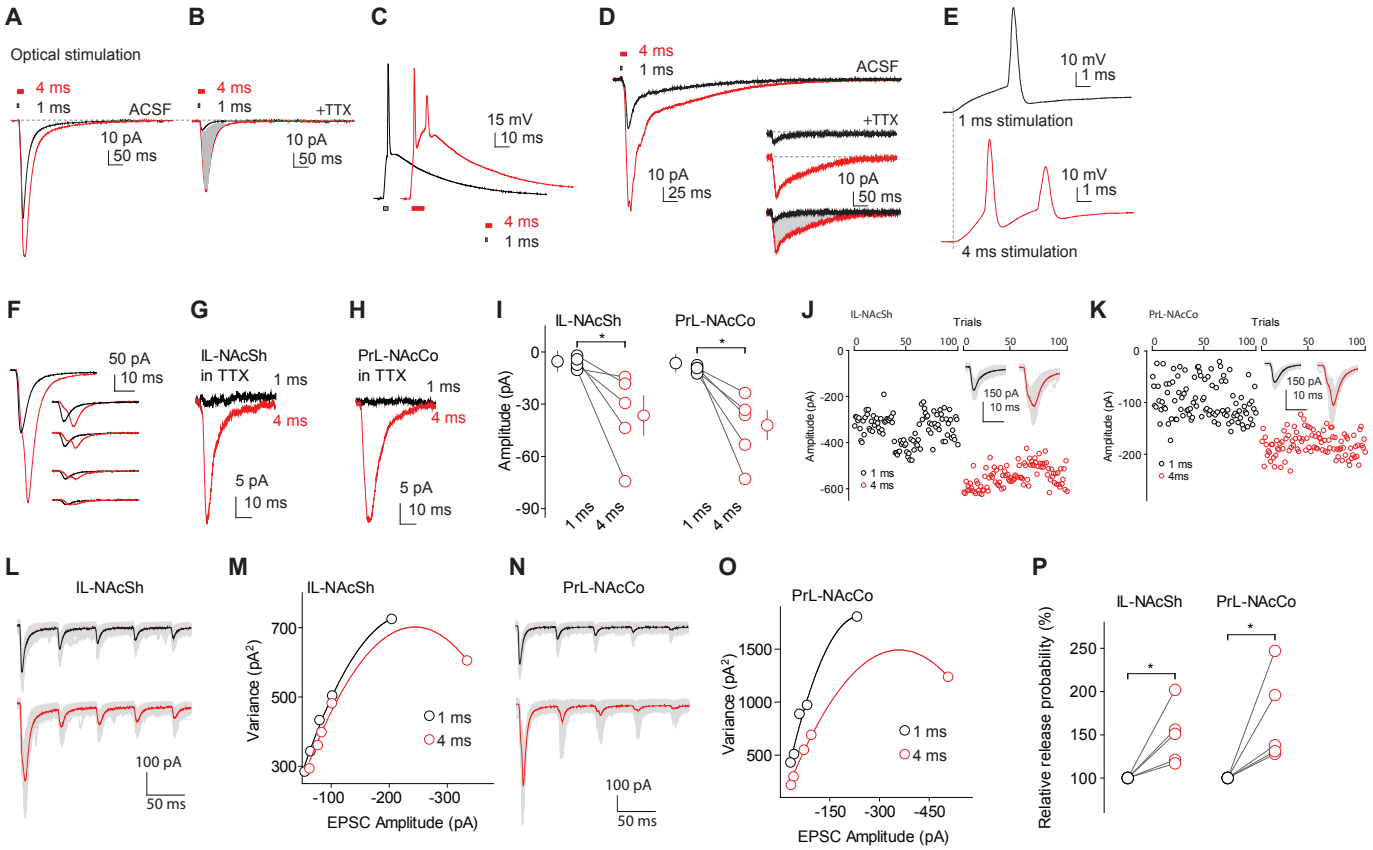
A
Optical stimulation
4 ms
1 ms
ACSF
10 pA
50 ms
B
4 ms
1 ms
+TTX
10 pA
50 ms
C
15 mV
10 ms
4 ms
1 ms
D
4 ms
1 ms
ACSF
10 pA
25 ms
+TTX
10 pA
50 ms
E
10 mV
1 ms
1 ms stimulation
10 mV
1 ms
4 ms stimulation
F
50 pA
10 ms
G
IL-NAcSh
in TTX
1 ms
4 ms
5 pA
10 ms
H
PrL-NAcCo
in TTX
1 ms
4 ms
5 pA
10 ms
I
IL-NAcSh
PrL-NAcCo
Amplitude (pA)
0
-30
-60
-90
1 ms
4 ms
J
IL-NAcSh
Trials
Amplitude (pA)
1 ms
4 ms
150 pA
10 ms
K
PrL-NAcCo
Trials
Amplitude (pA)
1 ms
4ms
150 pA
10 ms
L
IL-NAcSh
100 pA
50 ms
M
IL-NAcSh
Variance (pA²)
EPSC Amplitude (pA)
1 ms
4 ms
N
PrL-NAcCo
100 pA
50 ms
O
PrL-NAcCo
Variance (pA²)
EPSC Amplitude (pA)
1 ms
4 ms
P
IL-NAcSh
PrL-NAcCo
Relative release probability (%)

Fig. S2

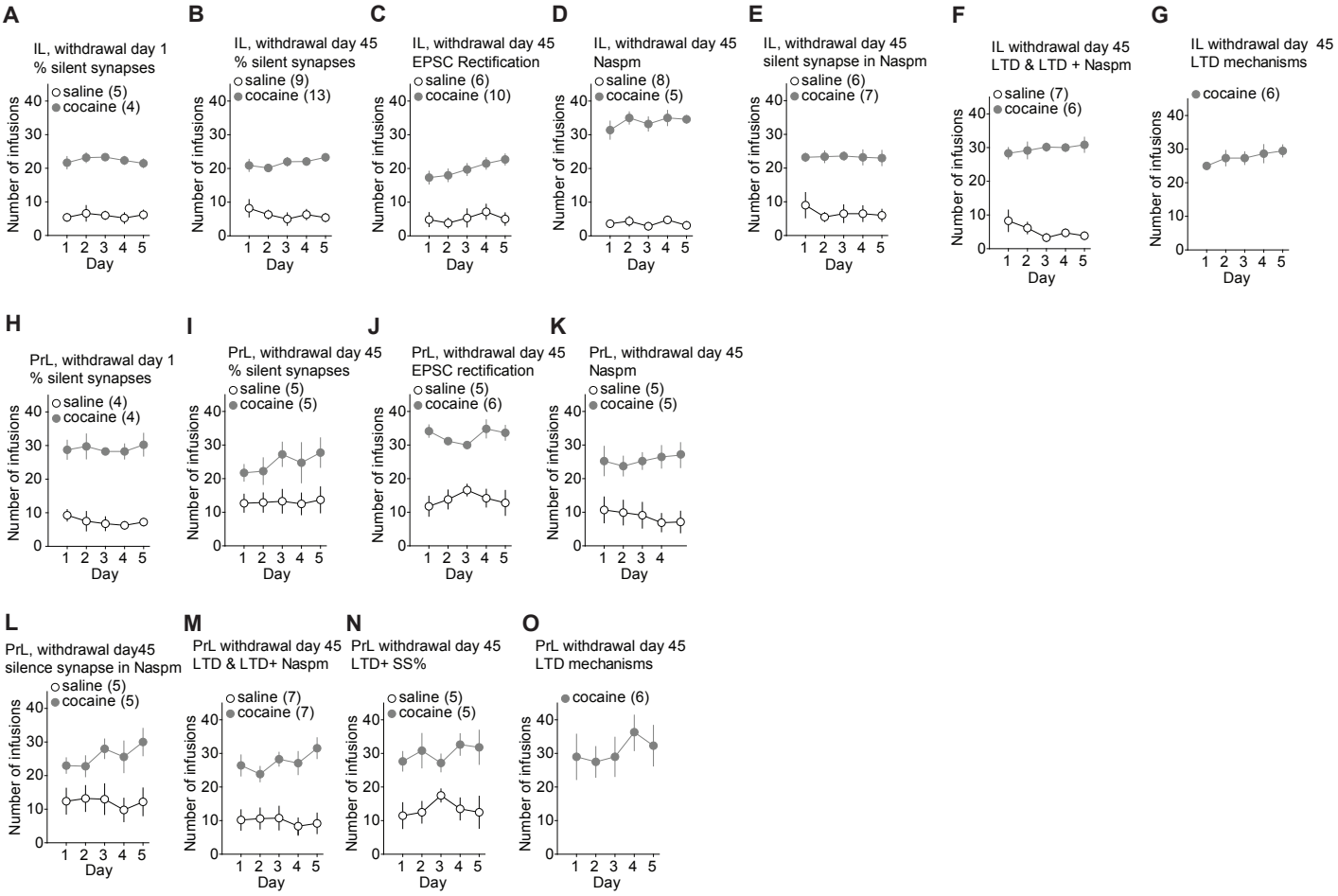
A
IL, withdrawal day 1
% silent synapses
saline (5)
cocaine (4)
B
IL, withdrawal day 45
% silent synapses
saline (9)
cocaine (13)
C
IL, withdrawal day 45
EPSC Rectification
saline (6)
cocaine (10)
D
IL, withdrawal day 45
Naspm
saline (8)
cocaine (5)
E
IL, withdrawal day 45
silent synapse in Naspm
saline (6)
cocaine (7)
F
IL withdrawal day 45
LTD & LTD + Naspm
saline (7)
cocaine (6)
G
IL withdrawal day 45
LTD mechanisms
cocaine (6)
H
PrL, withdrawal day 1
% silent synapses
saline (4)
cocaine (4)
I
PrL, withdrawal day 45
% silent synapses
saline (5)
cocaine (5)
J
PrL, withdrawal day 45
EPSC rectification
saline (5)
cocaine (6)
K
PrL, withdrawal day 45
Naspm
saline (5)
cocaine (5)
L
PrL, withdrawal day45
silence synapse in Naspm
saline (5)
cocaine (5)
M
PrL withdrawal day 45
LTD & LTD+ Naspm
saline (7)
cocaine (7)
N
PrL withdrawal day 45
LTD+ SS%
saline (5)
cocaine (5)
O
PrL withdrawal day 45
LTD mechanisms
cocaine (6)
Number of infusions
Day

Fig. S3

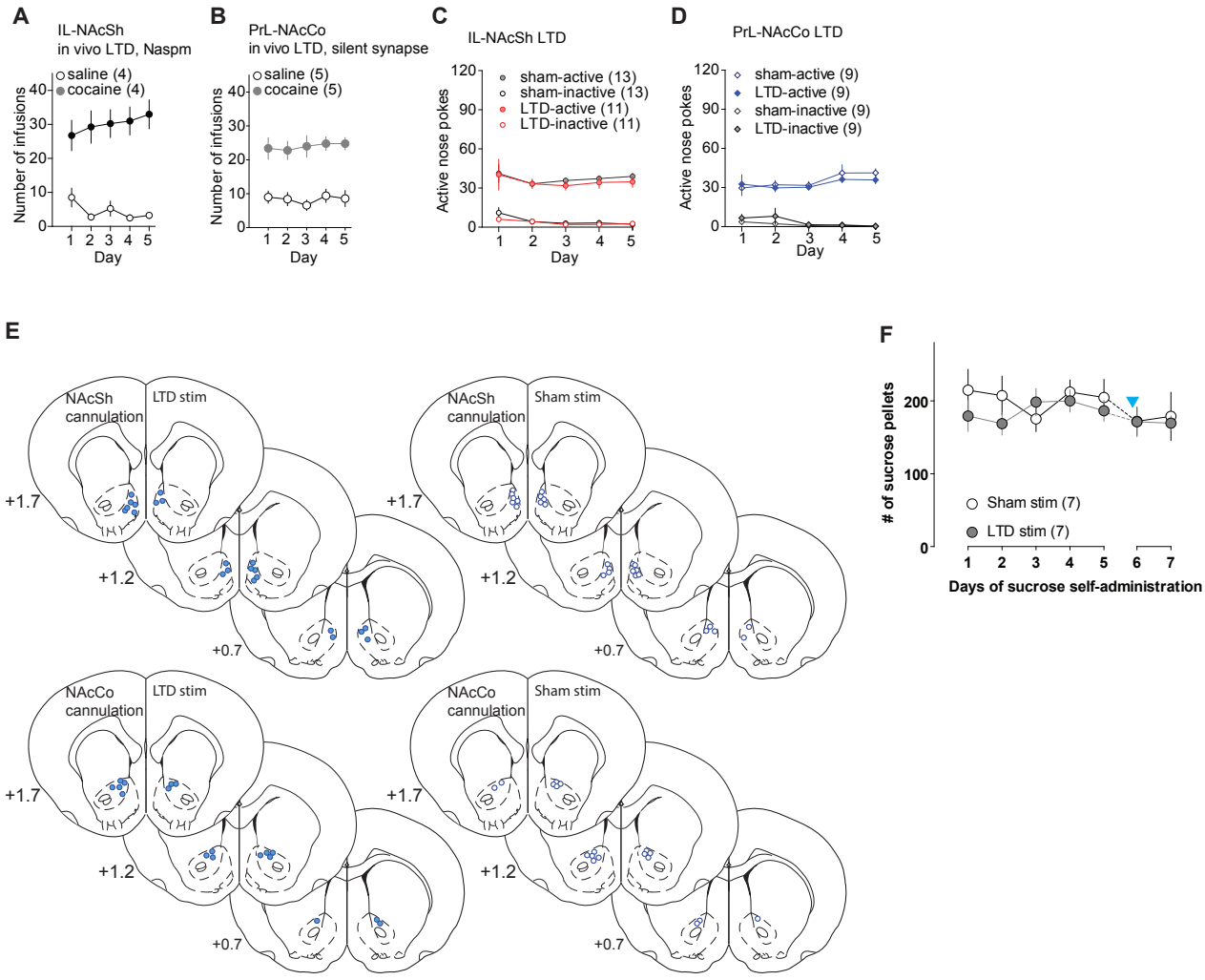
A
IL-NAcSh
in vivo LTD, Naspm
saline (4)
cocaine (4)
Number of infusions
Day
B
PrL-NAcCo
in vivo LTD, silent synapse
saline (5)
cocaine (5)
Number of infusions
Day
C
IL-NAcSh LTD
sham-active (13)
sham-inactive (13)
LTD-active (11)
LTD-inactive (11)
Active nose pokes
Day
D
PrL-NAcCo LTD
sham-active (9)
LTD-active (9)
sham-inactive (9)
LTD-inactive (9)
Active nose pokes
Day
E
NAcSh cannulation
LTD stim
Sham stim
NAcCo cannulation
+1.7
+1.2
+0.7
F
# of sucrose pellets
Sham stim (7)
LTD stim (7)
Days of sucrose self-administration

Fig. S4

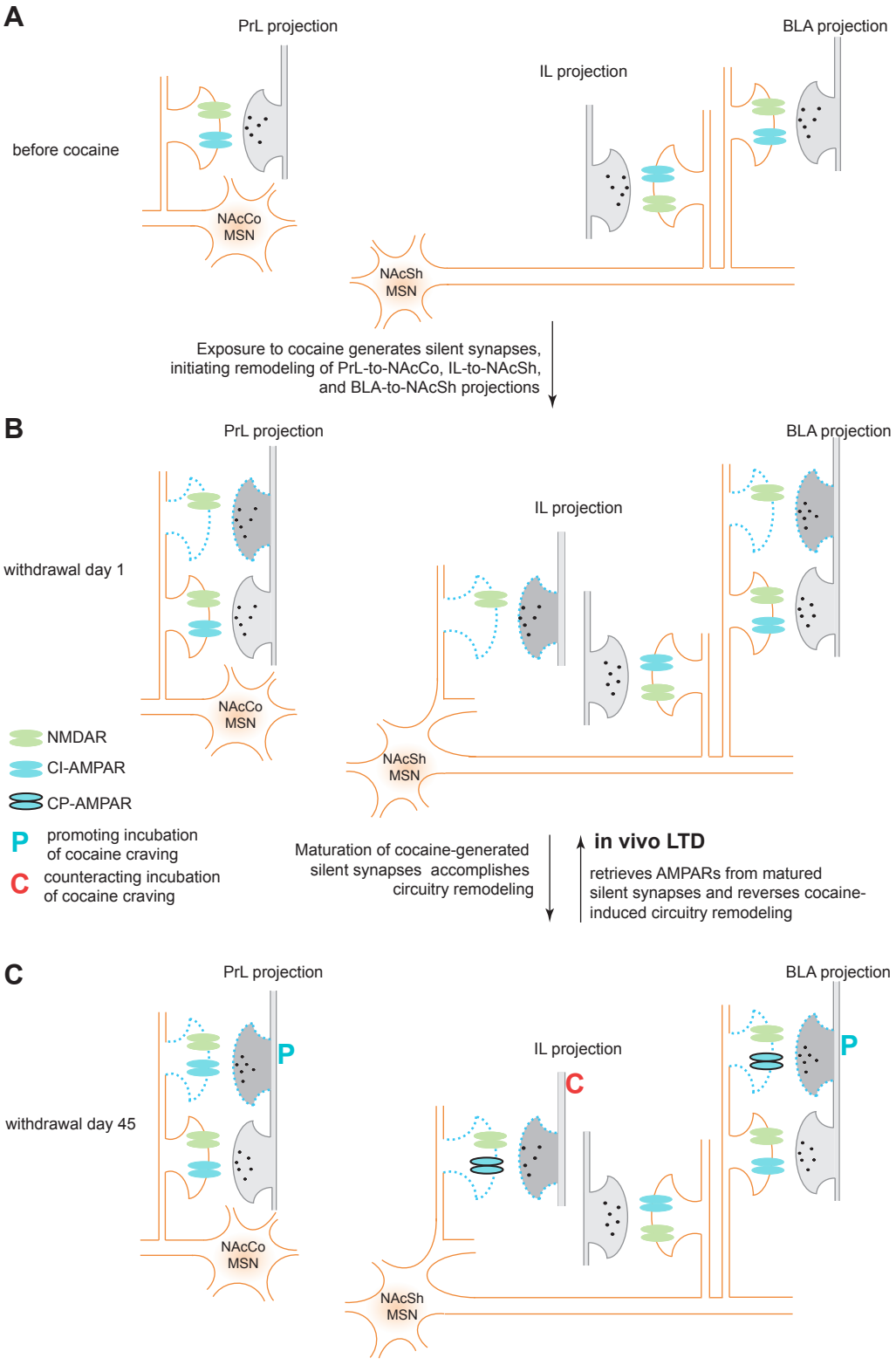
A
PrL projection
BLA projection
IL projection
before cocaine
NAcCo MSN
NAcSh MSN
Exposure to cocaine generates silent synapses, initiating remodeling of PrL-to-NAcCo, IL-to-NAcSh, and BLA-to-NAcSh projections
B
PrL projection
BLA projection
IL projection
withdrawal day 1
NAcCo MSN
NAcSh MSN
NMDAR
CI-AMPAR
CP-AMPAR
P promoting incubation of cocaine craving
C counteracting incubation of cocaine craving
Maturation of cocaine-generated silent synapses accomplishes circuitry remodeling
in vivo LTD
retrieves AMPARs from matured silent synapses and reverses cocaine-induced circuitry remodeling
C
PrL projection
BLA projection
IL projection
withdrawal day 45
P
C
P
NAcCo MSN
NAcSh MSN